https://doi.org/10.48048/tis.2023.5147

Optical Properties of Sol-Gel Deposited Barium Strontium Titanate ($Ba_xSr_{1-x}TiO_3$) Films

Sharmistha Lahiry

Faculty of Physics, Sri Aurobindo College, University of Delhi, Delhi, India

(Corresponding author's e-mail: sharmistha.lahiry@gmail.com)

Received: 9 July 2022, Revised: 10 August 2022, Accepted: 17 August 2022, Published: 15 March 2023

Abstract

Optical properties of sol-gel deposited Barium Strontium Titanate ($Ba_xSr_{1-x}TiO_3$, BST) thin films were studied to determine their suitability as light sensors. Crystallized BST films were formed by annealing in air at 700 °C for 1 h. Lattice parameters and grain sizes were determined for all the compositions. The band gap and refractive index values of the samples were determined from the optical transmission spectra for different compositions. Band gap of all the compositions were in the semiconductor range that would allow them to be used for photodiode and light sensor applications. Refractive index is reported for all the compositions.

Keywords: Barium Strontium Titanate films, Light sensors, Sol-gel method, Amorphous films, Crystallized films, Structural properties, Optical properties, Band gap, Refractive index

Introduction

Ferroelectric thin films deposited by various methods have been widely investigated for various applications such as in dynamic random access memories, capacitor devices, microwave tunable phase array antennas, waveguides, electro-optical devices, thermistors and many more [1-4].

Recently, Barium Strontium Titanate ($Ba_xSr_{1-x}TiO_3$, BST) thin films have been investigated as photodiodes in light and temperature sensors [5-7], dye-sensitized solar cells [8], and glucose sensors [9]. Faridawati *et al.* [6] investigated the possibility of 2 composition of BST x = 0.25 and x = 0.75 deposited on ITO (Indium tin oxide) for light sensor applications. Barium Strontium Titanate ($Ba_xSr_{1-x}TiO_3$, BST) has an optical absorbance in the ultraviolet-visible-infrared region, making it excellent for temperature and light sensors such as photodiodes [5,6].

Generally, only 1 or 2 compositions of BST have been investigated for sensor applications in literature. In this paper, we investigate the viability of BST for light sensor applications for the entire range of compositions with x varying from 0.0 (Strontium Titanate) to 1.0 (Barium Titanate) by examining its optical properties like band gap and refractive index.

Materials and methods

Barium Strontium Titanate ($Ba_xSr_{1-x}TiO_3$) films of different compositions (x = 0.0, 0.2... 1.0) were deposited by sol-gel method on quartz substrate. Barium-ethyl-hexanoate ($Ba(C_8H_{15}O_2)_2$), Strontium-ethyl-hexanoate ($Sr(C_8H_{15}O_2)_2$) and Titanium(IV)-isopropoxide ($TiC_{12}H_{28}O_4$) were used as precursors. Ethanol was used as the solvent. Requisite moles of Barium-ethyl-hexanoate and Strontium-ethyl-hexanoate were separately dissolved in ethanol and then mixed together. To this solution Titanium-isopropoxide was added. Two additives namely, acetyl-acetone and formamide were added to the solution and filtered to prepare the final stock solution. Films were deposited on quartz substrate by spin coating. The method of preparing the sample was described in earlier paper in detail [10]. Films obtained in the process were amorphous in structure but they are converted into polycrystalline structure after annealing in air for 1 h. The thickness of the films was measured by DEKTAK (Model IIA) surface profiler. The crystallographic orientation of the films was analysed by using a Philips (expert model PW 1830) X-ray diffractometer. The optical characterization of the films was carried out by measuring the transmission for films deposited on quartz substrate in the wavelength range of 190 to 900 nm using Shimadzu UV-260 spectrophotometer. A Jeol (model JSM-840) scanning electron microscope was used to investigate the surface topographical features of the films.

$Ba_xSr_{1-x}TiO_3$ (BST) films of composition x = 0.0, 0.2, 0.4, 0.6, 0.8, 1.0 having thicknesses of the order of ~0.5 μm deposited on quartz substrate were used for optical measurements. The transmission spectra were noted for both amorphous and crystalline films for all the compositions.

Results and discussion

Structural studies

Crystallographic orientations were studied from X-ray diffraction (XRD) patterns and surface morphologies were studied from the scanning electron micrographs (SEM). **Figure 1** shows the X-ray diffraction (XRD) patterns, of crystallized sol-gel deposited BST film on quartz substrate for compositions x= 0.0, ... 1.0. **Figure 2** shows the scanning electron micrographs of the crystallized BST samples for various compositions. The as-fired films of $Ba_xSr_{1-x}TiO_3$ were transparent, smooth, crack free and were found to adhere strongly to the quartz substrates. Films annealed at 700 °C were uniform, crack free and exhibited polycrystalline structure as shown by the SEM photographs. XRD patterns of films deposited on quartz exhibit similar pattern as observed for films deposited on Pt/Si [11,12]. The XRD patterns showed that the BST films deposited on quartz were polycrystalline in nature with (110) peak.

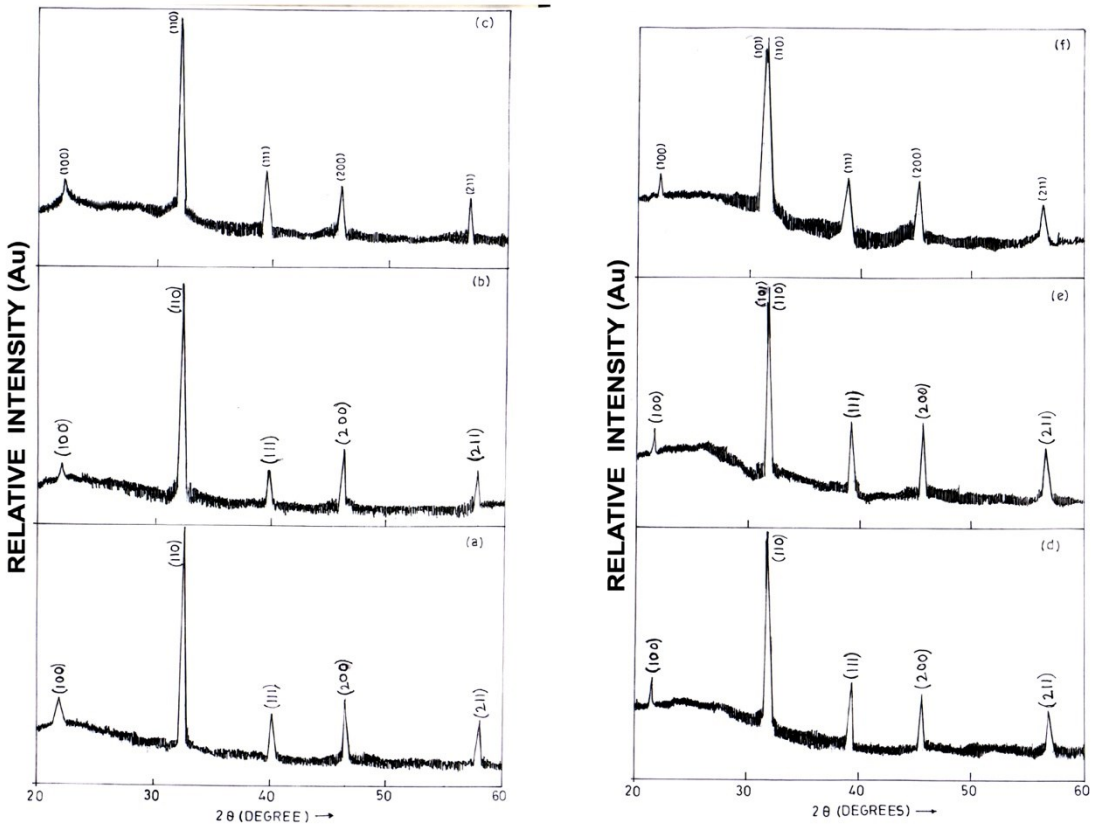

Figure 1 The X-ray diffraction patterns of sol-gel deposited BST film on quartz for the compositions (a) x = 0.0, (b) x = 0.2, (c) x = 0.4, (d) x = 0.6, (e) x = 0.8, (f) x = 1.0

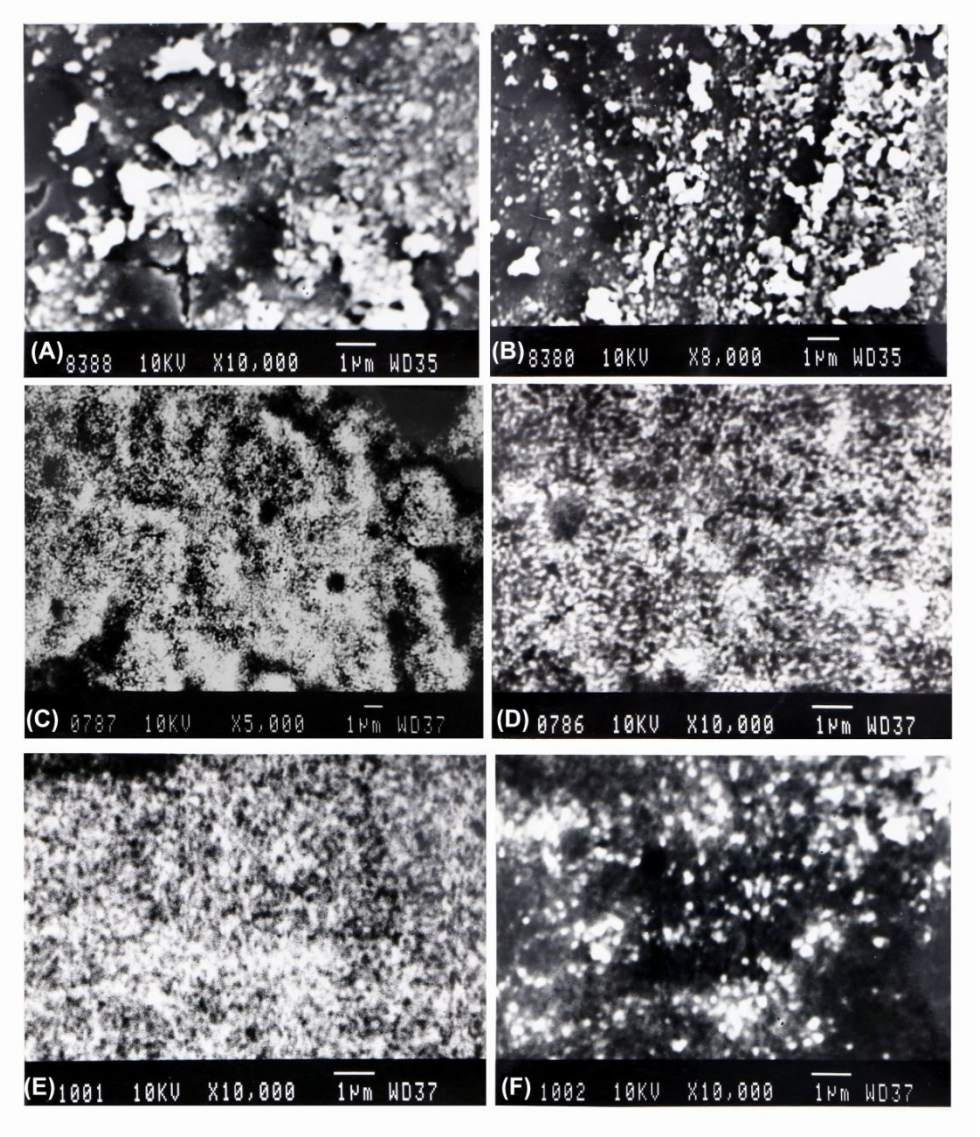

Figure 2 SEM photographs of sol-gel deposited BST film for the compositions (A) x = 0.0, (B) x = 0.2, (C) x = 0.4, (D) x = 0.6, (E) x = 0.8, (F) x = 1.0

(110) peak at 32 ° as the most dominant peak. XRD data show that the compositions x = 0.0, 0.2, 0.4, 0.6 are in the cubic phase and the compositions x = 0.8 and x = 1.0 are in the tetragonal phase. **Table 1** lists the lattice constant for various compositions. Lattice constants for films deposited on platinised silicon (Pt/Si) reported in our earlier papers also show similar values [11]. **Table 1** show that our values are well within the range of lattice constant values reported by other workers [13-15]. However, for the complete composition range of $Ba_xSr_{1-x}TiO_3$ the lattice constants *a* and *c* of thin films were larger than that of the bulk [13] material.

The grain size was calculated from the X-ray diffraction pattern by using the Full Width at Half Maximum (FWHM) of the dominant peak using Scherrer's relation [16].

$$D = \frac{0.94\lambda}{B_0 \cos\theta} \quad (1)$$

where B_0 is the FWHM of the peak, λ is the wavelength of the X-ray beam and θ is the diffraction angle. **Table 1** lists the grain size for various compositions. The grain sizes of all the films are in the range of 20- 50 nm. **Table 1** show that the grain size decreases with increase in Barium content (x) or it can as well be stated that grain size increases with increase in Strontium content (1-x). SEM photographs also

show a similar pattern (**Figure 2**). There was a grain size distribution when it was calculated from SEM photographs. For a particular composition x = 0.4, the grain size calculated from SEM data varied from 35 to 48 nm. However, the average value was close to that estimated from XRD data (**Table1**).

Table 1 Thickness of the films (d_m), lattice constants (*a, c*) and grain size (D) for various compositions (x) of various compositions of $Ba_xSr_{1-x}TiO_3$.

x	d_m (μm) ±0.01	*a* (nm) ±0.0001	*c* (nm) ±0.0001	grain size D (nm) ±0.1
0.0	0.54	0.3916		53.9
0.2	0.52	0.3940		43.2
0.4	0.53	0.3954		39.2
0.6	0.50	0.3966		35.5
0.8	0.54	0.3994	0.4012	28.7
1.0	0.54	0.4004	0.4047	21.5

The increase in grain size with increase in Strontium content was observed by Kawano *et al.* [17] for their sputtered films, Kim *et al.* [18] for their sol-gel films. The differences in grain sizes in solid solution of BST with increasing Strontium (Sr) concentration have been explained by Kawano *et al.* [17] from their TEM (tunnelling electron micrographs) data. They assumed that the crystallization in $BaTiO_3$ amorphous samples was essentially controlled by nucleation process while for $SrTiO_3$ the microstructure after crystallization was characterized mostly by large globular crystallites [17]. In the solid solution of $Ba_xSr_{1-x}TiO_3$, an increase in grain size with increase in Sr content is considered to change from fine equiaxed crystallites in $BaTiO_3$ to coarse globular crystallites in $SrTiO_3$. Further, the crystallization of $SrTiO_3$ sample was followed by nucleation and growth of grain size. According to Kawano *et al*. [17], an enhanced diffusion could lead to increased grain growth as the Sr content increases since the ionic radius of Sr^{2+} is less than that of Ba^{2+}. Our observations from the SEM of the solid solution of BST are similar to TEM of Kawano *et al.* [17] and we propose the above mechanism for increase in grain size as the concentration of Sr increases. The thicknesses of the films for the various compositions are also reported in **Table 1**.

Optical studies

Optical studies were carried out for $Ba_xSr_{1-x}TiO_3$ (BST) films of compositions x = 0.0, 0.2, 0.4, 0.6, 0.8, 1.0. **Figures 3** and **4** show the optical transmission spectra of the amorphous and crystalline films respectively on quartz substrates. The transparency of the amorphous films was ≅ 95 % and decreased to ≅ 90 % for the crystalline films for all the compositions. Post deposition annealing strongly affected the optical transmission spectra. Annealing in air moved the absorption edge towards lower photon energy. But the shift was pronounced in the case of Barium titanate (x = 1.0) compared to Strontium titanate (x = 0.0). The transparencies of our BST films are comparable to those of Tcheliebou *et al*. [19] prepared by pulsed laser deposition by Pasierb *et al.* [20] by rf sputtering method. This shows that the optical quality of the films prepared by sol-gel method were comparable with those prepared by other methods.

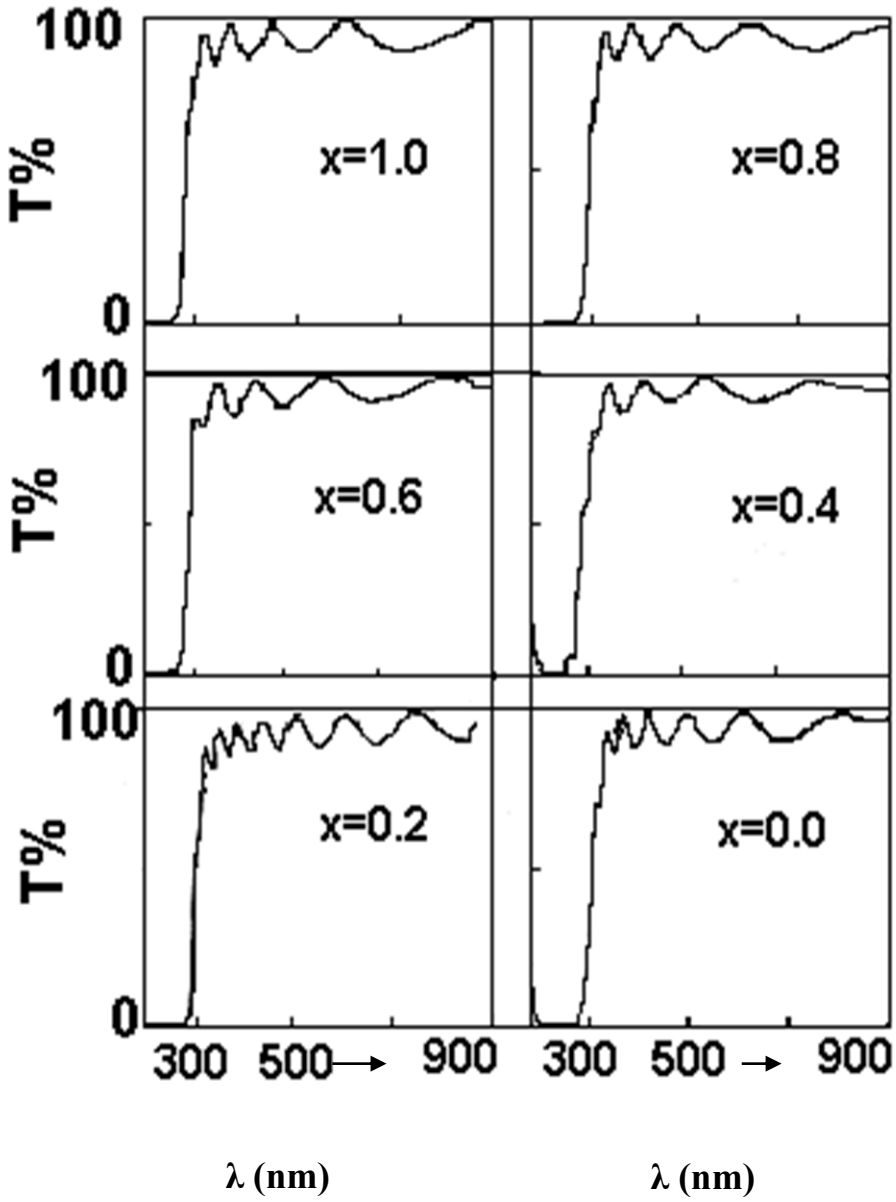

Figure 3 The optical transmission spectra of the amorphous $Ba_xSr_{1-x}TiO_3$ films on quartz substrates for the composition x = 0.0, 0.2, 0.4, 0.6, 0.8, 1.0.

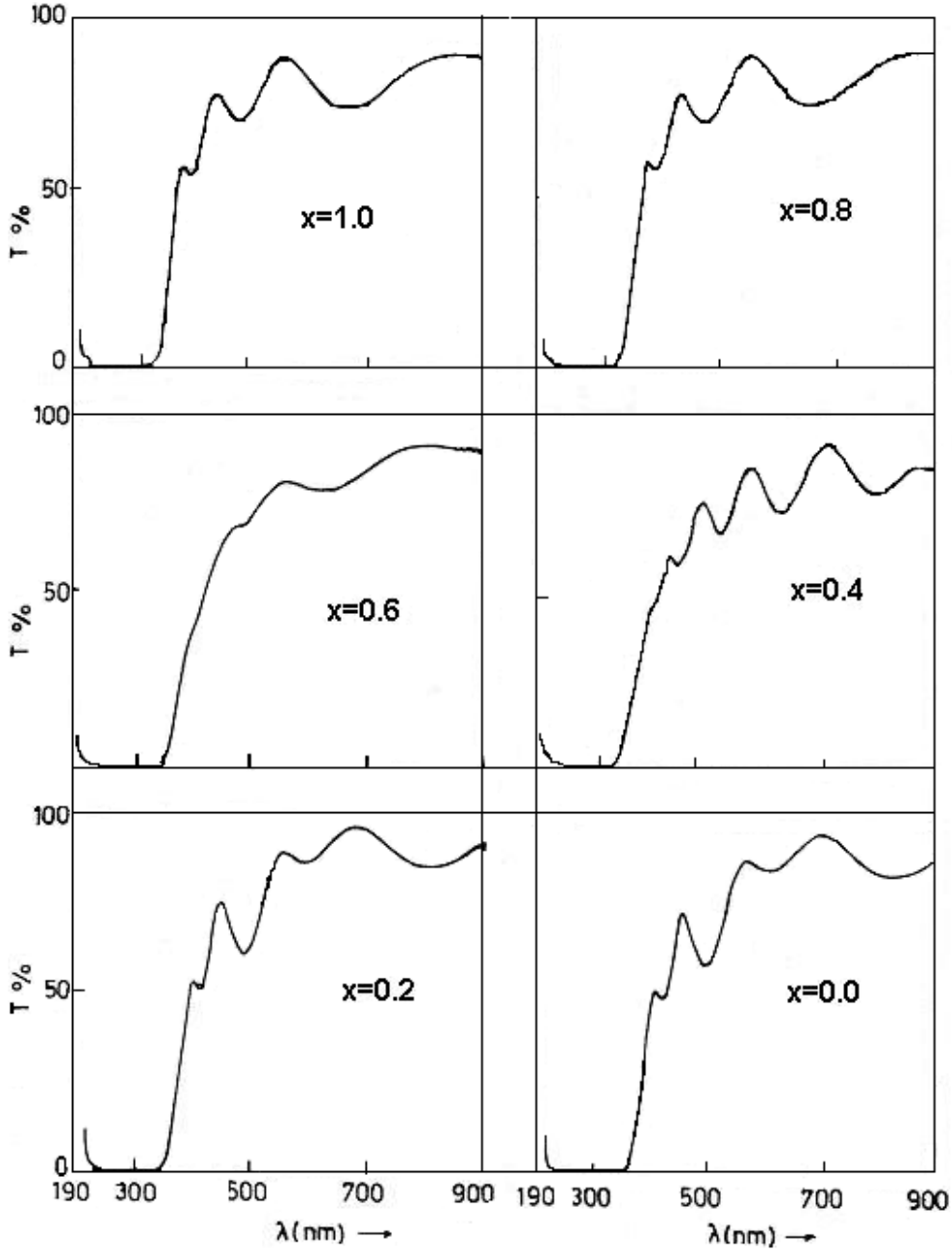

Figure 4 The optical transmission spectra of the crystalline $Ba_xSr_{1-x}TiO_3$ films on quartz substrates for the composition x = 0.0, 0.2, 0.4, 0.6, 0.8, 1.0.

The band gap (E_g) of the films was determined using the relation:

$$\alpha = \left(h\nu - E_g\right)^{1/2} \tag{2}$$

where α is the absorption coefficient and $h\nu$ is photon energy. The plots of α^2 vs $h\nu$ for the amorphous and crystalline films are given in **Figures 5** and **6**, respectively. The calculated band gap of all the films are reported in **Table 2**. The band gap of the amorphous films was greater than that of the crystalline films for all the compositions. For the sol-gel derived amorphous films, the band gap continuously increased from 4.12 eV (for x = 0.0) to 4.26 eV (for x = 1.0). For the crystalline films, the band gaps for

x = 0.0 and 1.0 are 3.65 and 3.61, respectively which were higher than that obtained for other solid solution compositions. Band gap does not show continuous decrease but exhibits a minimum of 3.55 eV at x = 0.6. Band gaps of all the compositions of BST lie in the semiconductor range which makes them suitable for light sensor applications [6,7].

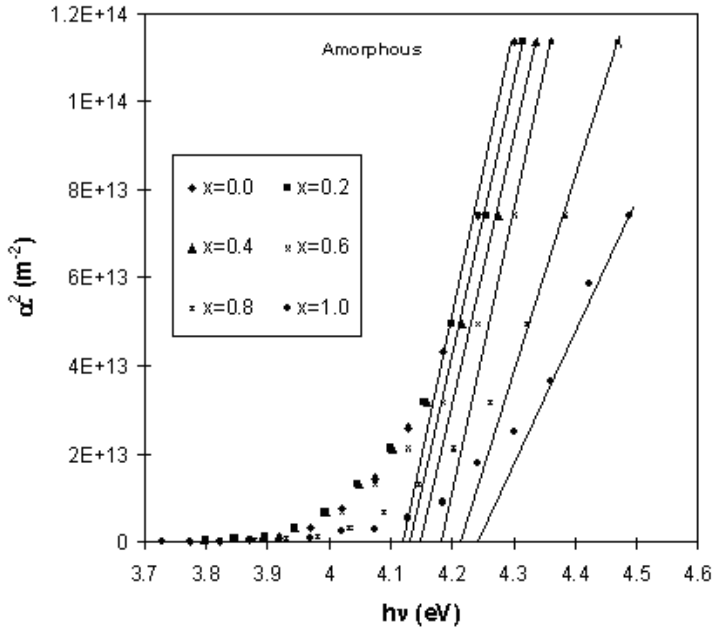

Figure 5 Variation of square of absorption coefficient with photon energy for amorphous $Ba_xSr_{1-x}TiO_3$ films on quartz substrates for the compositions x = 0.0, 0.2, 0.4, 0.6, 0.8, 1.0.

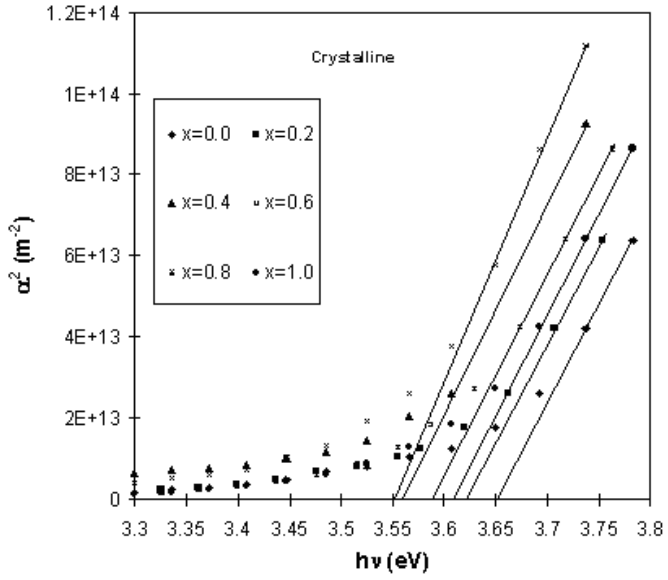

Figure 6 Variation of square of absorption coefficient with photon energy for crystalline $Ba_xSr_{1-x}TiO_3$ films (films annealed at 700 °C) on quartz substrates for the compositions x = 0.0, 0.2, 0.4, 0.6, 0.8, 1.0.

Faridawati *et al.* [6] reported a band gap of 3.4 and 3.3 eV for BST films on ITO (Indium tin oxide) of composition x = 0.75 and x = 0.25, respectively. Iskander *et al.* [7] obtained band gap varying between 2.54 to 3.19 eV for BST films of composition x = 0.5 deposited on p-Si for annealing time varying

between 8 to 29 h at 850 °C. Band gaps of the crystallized films were smaller than those of the amorphous films which make them better suited for light sensor applications. For the crystallized films, band gap values of the end members were greater than those of the solid solutions. This makes these compositions better suited for light sensor applications. For our films, band gap values in the composition range of x = 0.4 to x = 0.6 were minimum and did not show much composition variation which makes them better for light sensor applications. However, properties of thin films are known to vary with the fabrication method and preparation conditions [19,20].

The refractive index (n) of the amorphous and the crystalline films were calculated from the transmittance spectra by using the fringe envelope method [21,22]. The values of the refractive index for different compositions are reported in **Table 2**. The refractive index for the amorphous films lies between 1.99 (for x = 0.0) and 1.97 (for x = 1.0). For the crystalline films, a maximum refractive index of 2.16 was obtained for x = 0.6. For x = 0.0 and 1.0 refractive index values of 2.14 and 2.13, respectively were obtained. Similar values of refractive index were reported by other workers [6,19,20,23]. Faridawati *et al.* [6] reported a refractive index of 2.31 and 2.30 for their films of composition x = 0.25 and 0.75, respectively. The refractive index value indicates how well a film can transport light while also acting as an anti-reflection layer [6]. The ability to transmit radiation improves as the refractive index of the films decreases [6]. Hence, amorphous films may be better for use as anti-reflection layer.

Table 2 Band gap (E_g), refractive index (n) at λ=500nm, of the amorphous and crystalline films of composition x=0.0, 0.2, 0.4, 0.6, 0.8, 1.0.

x	E_g (eV) ±0.01 (amorphous)	E_g (eV) ±0.01 (crystalline)	*n* ±0.01 (amorphous)	*n* ±0.01 (crystalline)
0.0	4.12	3.65	1.99	2.14
0.2	4.13	3.63	1.98	2.15
0.4	4.16	3.56	1.97	2.15
0.6	4.18	3.55	1.97	2.16
0.8	4.21	3.59	1.97	2.15
1.0	4.26	3.61	1.97	2.13

Conclusions

Values of band gap and refractive index for various compositions of BST were determined for both amorphous and crystalline films. The band gap values exhibit the following salient characteristics. For the amorphous films they increased from 4.12 eV for x = 0.0 to 4.26 eV for x = 1.0, while for the crystalline films the corresponding values were 3.65 eV and 3.61 eV for x = 0.0 and 1.0, respectively. However, for the crystalline films the band gap values did not decrease continuously, instead, a minimum value of 3.55 eV at x = 0.6 was obtained. These values indicated that the films have band gap in the semiconductor range. This makes them suitable for light sensor applications and as photodiodes. The band gap of the crystalline films was smaller than that of the amorphous films for all solid solution compositions. This shows that crystalline films would be better suited for light sensor applications. Also the band gap of the end members (x = 0.0 and x = 1.0) were greater than various solid solution compositions which makes the solid solution compositions better suited for light sensors applications. Band gap values of our films in the composition range x = 0.4 to x = 0.6 showed minimum band gap and also did not show much variation with composition which makes them best suited for light sensor applications.

References

[1] FL Traversa, F Bonani, YV Pershin and MD Ventra. Dynamic computing random access memory. *Nanotechnology* 2014; **25**, 285201.

[2] LC Sengupta and S Sengupta. Novel ferroelectric materials for phased array antennas. *IEEE Trans. Ultrason. Ferroelectrics Freq. Contr.* 1997; **44**, 792-7.

[3] AO Outzourhit, JU Trefny, T Kito and B Yarar. Tunability of the dielectric constant of $Ba_{0.1}Sr_{0.9}TiO_3$ ceramics in paraelectric state. *J. Mater. Res*. 1995; **10**, 1411-7.

[4] NA Vainos and MC Gower. High-fidelity phase conjugation and real-time orthoscopic three dimensional image projection in $BaTiO_3$. *J. Opt. Soc. Am. B* 1991; **8**, 2355.
[5] Irzaman, R Siskander, Aminullah and H Alatas. Characterization of Barium Strontium Titanate films as light and temperature sensors and its implementation on automatic drying system model. *Integrated Ferroelectrics Int. J*. 2016; **168**, 130-50.
[6] F Faridawati, AY Rohedi, E Minarto, G Yudoyono, T Widihartanti, YH Pramono and N Yuningtyas. The comparison of optical properties between $Ba_{0.25}Sr_{0.75}TiO_3$ and $Ba_{0.75}Sr_{0.25}TiO_3$ thin films as the light sensor application. *J. Phys. Conf. Ser.* 2021; **1825**, 012079.
[7] J Iskander, H Syafutra, J Juansah and Irzaman. Characterization of electrical and optical properties on ferroelectric photodiode of Barium Strontium Titanate ($Ba_{0.5}Sr_{0.5}TiO_3$) films based on annealing time difference and its development as light sensor on satellite sensor technology. *Proc. Environ. Sci.* 2015; **24**, 324-8.
[8] V Kavitha, V Raghavendran, N Sethupathi, S Sagadevan, V Sasirekha, JM Pearce and J Mayaandi. Microwave assisted synthesized Gadolinium doped Barium Strontium Titanate nanostructures: structural and optical properties for DSSC applications. *Malays. Nano Inter. J.* 2021; **1**, 71-82.
[9] EK Palupi, H Alatas, Irzaman, Y Suryana, A Aridarma, R Umam, BB Andriana and H Sato. Optimization of optical properties of $Ba_{0.2}Sr_{0.8}TiO_3$ thin films for a glucose sensor implementation. *Biomed. Spectros. Imag*. 2020; **9**, 63-71.
[10] S Lahiry, V Gupta, K Sreenivas and A Mansingh. Dielectric properties of sol-gel derived Barium-Strontium-Titanate ($Ba_{0.4}Sr_{0.6}TiO_3$) thin films. *IEEE Trans. Ultrason. Ferroelectrics Freq. Contr.* 2000; **47**, 854-60.
[11] S Lahiry and A Mansingh. Dielectric properties of sol-gel derived Barium Strontium Titanate thin films. *Thin Solid Films* 2008; **516**, 1656-62.
[12] S Lahiry and A Mansingh. Electric field dependence of dielectric constant of the sol-gel deposited $Ba_xSr_{1-x}TiO_3$ film - thermodynamic analysis. *Ferroelectrics* 2004; **306**, 37-54.
[13] H Landolt and R Börnstein. *Landolt-bornstein: Numerical data and functional relationship in science technology - New series*. Springer Verlag, Berlin, Germany, 1982, p. 296.
[14] H Kobayashi and T Kobayashi. Hetroepitaxial growth of quaternary $Ba_xSr_{1-x}TiO_3$ thin films by ArF excimer laser ablation. *Jpn. J. Appl. Phys*. 1994; **33**, L533.
[15] TS Kim, CH Kim and MH Oh. Structural and electrical properties of rf-magnetron-sputtered $Ba_{1-x}Sr_xTiO_3$ thin films on indium-tin-oxide-coated glass substrate. *J. Appl. Phys*. 1994; **75**, 7998.
[16] BD Cullity. *Elements of x-ray diffraction*. 2nd eds. Addison Wesley, Massachusetts, United States, 1978, p. 102.
[17] H Kawano, K Morii and Y Nakayama. Effects of crystallization on structural and dielectric properties of thin amorphous films of (1-x) $BaTiO_3$-x$SrTiO_3$ (x = 0 - 0.5, 1.0). *J. Appl. Phys.*1993; **73**, 5141.
[18] J Kim, SI Kwun and JG Yoon. Precursor dependent properties of $Ba_{1-x}Sr_xTiO_3$ thin films fabricated by sol-gel method. *In*: Proceedings of the 9th International Symposium on the Application of Ferroelectrics, Pennsylvania, United States. 1994. p. 423-6.
[19] F Tcheliebou, S Ryu, CK Hong, WS Park and S Baik. On the microstructure and optical properties of $Ba_{0.5}Sr_{0.5}TiO_3$ films. *Thin Solid Films* 1997; **305**, 30-4.
[20] P Pasierb, S Komornicki and M Radecka. Structural and optical properties of $Sr_{1-x}Ba_xTiO_3$ thin films prepared by rf-sputtering. *Thin Solid Films* 1998; **324**, 134-40.
[21] JC Manifacier, J Gasiot and J P Fillard. A simple method for determination of the optical constants n, k and thickness of a weakly absorbing thin film. *J. Phys. E* 1997; **9**, 1002.
[22] OS Heavens. *Optical properties of thin solid films.* Dover Publication, New York, United States, 1965.
[23] I Suzuki and M Eijima. Spectroscopic ellipsometry characterization of $Ba_{0.7}Sr_{0.3}TiO_3$ thin films prepared by sol-gel method. *Thin Solid Films* 1998; **313-314**, 214-17.